

An iterative tangential interpolation algorithm for model reduction of MIMO systems

Jared Jonas and Bassam Bamieh, *Fellow, IEEE*

Abstract—We consider model reduction of large-scale multi-input, multi-output (MIMO) systems using tangential interpolation in the frequency domain. Our scheme is related to the recently-developed Adaptive Antoulas–Anderson (AAA) algorithm, which is an iterative algorithm that uses concepts from the Loewner framework. Our algorithm has two main features. The first is the use of freedom in interpolation weight matrices to optimize a proxy for an H_2 system error. The second is the use of low-rank interpolation, where we iteratively add low-order interpolation data based on several criteria including minimizing maximum errors. We show there is freedom in the interpolation point selection method, leading to multiple algorithms that have trade-offs between computational complexity and approximation performance. We prove that a weighted H_2 norm of a representative error system is monotonically decreasing as interpolation points are added. Finally, we provide computational results and some comparisons with prior work, demonstrating performance on par with standard model reduction methods.

Index Terms—Adaptive Antoulas–Anderson algorithm, computational methods, linear systems, Loewner framework, model order reduction, moment matching, optimization, rational interpolation, reduced order modeling

I. INTRODUCTION

Interpolatory model reduction methods have become an increasingly important tool in model-order reduction for many reasons, particularly their computational benefits [1]. This is particularly important in the context of large-scale linear systems that may be very sparse, for example in systems derived from finite-difference or finite-element discretizations of phenomena represented by partial differential equations like fluid or structure mechanics [2] [3]. There are two important sub-classifications of interpolatory methods, which are model matching methods and rational Krylov methods [1]. Essentially, moment matching methods are a group of methods that create systems which match the given system’s transfer function (or its derivatives) at a selected number of points in the complex plane.

Moment matching for linear systems can be thought of as fitting a rational interpolant to frequency data, thus algorithms that construct rational interpolants from data can be used for model order reduction. One such example of this is the Loewner framework originally introduced by Antoulas and Anderson [4], and was expanded upon thereafter [5].

Jared Jonas and Bassam Bamieh are with the department of Mechanical Engineering at University of California, Santa Barbara, {jjjonas,bamieh}@ucsb.edu. This work is partially supported by NSF award ECCS-2453491.

From frequency response data, one can construct a state-space representation by forming certain matrices, namely the so-called Loewner matrix. We will expand on this more when we talk about the Loewner framework for MIMO systems.

Unlike algorithms where the interpolation points are pre-selected, the AAA (Adaptive Antoulas–Anderson) algorithm [6] introduced by Trefethen and coauthors incorporates a recursive algorithm for selecting the next interpolation point at each step. It can be thought of as a greedy version of the scalar Loewner framework that iteratively builds up the interpolant point-by-point until the resulting rational function approximates the input data well. At each step, the AAA algorithm selects the next interpolation point to be the point at which a certain error is maximized, then readjusts free parameters in the system to further minimize the error across the rest of the points. Though introduced in the context of rational approximation, given a large set of points in the complex plane and the frequency response evaluated at those points, the AAA algorithm has proved itself able to generate satisfactory reduced order transfer functions for SISO systems.

For both the Loewner framework and the AAA algorithm, there are generalizations that apply to MIMO systems. For example, the Loewner framework has been generalized to MIMO systems with the use of tangential interpolation functions, which may be left- or right-tangential interpolants [5] [7]. A function R is said to be a *right-tangential interpolating function* if it satisfies the property $R(s_i)V_i = G(s_i)V_i$ at each interpolation point s_i , where V_i is a full column rank matrix. Similarly, a function is said to be a *left-tangential interpolating function* if it satisfies the property $U_i^*R(s_i) = U_i^*G(s_i)$, where U_i is a full column rank matrix. With the generalized Loewner framework, a reduced order system can be constructed by forming two Loewner matrices and performing a singular value decomposition (SVD) on each matrix, from which one can derive the coefficient matrices for a state space realization of a low order approximation. This is computationally efficient and thus is very useful for large, sparse systems. Though we will not discuss it in this paper, a related algorithm, known as the iterative rational Krylov method (IRKA), is an iterative Loewner framework algorithm that shifts the interpolation points iteratively until they satisfy some H_2 optimality conditions [8] [7].

There have been several attempts at adapting the AAA algorithm for use in MIMO system reduction. For example, the block-AAA algorithm adjusts the interpolant to use matrix-valued functions and “block” interpolates (i.e. fully interpolates) the matrix-valued functions at each interpolation point [9].

This system's order grows by either the number of inputs or the number of outputs every iteration, as shown in our prior work [10]. Benner et al. [11] introduced tangential-AAA, which uses tangential-interpolation from the Loewner framework to create a system that grows by a constant every iteration and thus performs better than the block-AAA algorithm [11].

In this work, we aim to develop an algorithm based on our prior work and other AAA-like algorithms that is suitable for model reduction of MIMO linear, time-invariant (LTI) systems. Available model reduction methods based on the AAA algorithm require a large set of evaluation points, and their performance is closely linked to both the number of points and the distribution of said points. The resulting systems from these methods tend to be unstable, even when the system to be approximated is stable. In prior work [10], we began to address this with the system-AAA algorithm, which may be thought of as the limiting case of the block-AAA algorithm with an infinite number of evaluation points on the imaginary axis, eliminating the need for these evaluation points. This algorithm gave satisfactory results when reducing single input, single output (SISO) systems, but performed relatively poorly when reducing MIMO systems, especially when the number of inputs and/or outputs is large. This begat the low-rank approximation algorithm introduced at the end of our prior work, which was a cursory look at some of the ideas we flesh out in this manuscript.

In this paper we present an algorithm that generalizes and improves upon our prior work while laying out important theoretical implications. The family of algorithms we introduce efficiently produces well-performing models in the MIMO case with good empirical stability characteristics and performance which matches standard model reduction algorithms. We summarize these results in the following Section II. Section III carefully catalogs the transfer functions and state space realizations for systems that appear in this paper, as there are important observability/controllability and MIMO pole/zero cancellation issues to keep track of. Sections IV and V form the bulk of our contribution. In Section IV we show how the free parameters in the interpolant (the weight matrices) can be used to minimize a measure of H_2 system error. The optimization problem has an explicit solution through an eigenvalue problem involving the weight matrices and certain system Gramians. We also show that this system error is monotonically decreasing across iterations. Section V introduces three variations of the interpolation point selection algorithm, as well as the selection of approximation rank at said points. Section VI gives computational examples of the performance of our algorithms as well as other model reduction algorithms and provides some commentary on the results and algorithms as a whole.

II. PROBLEM FORMULATION AND MAIN RESULTS

We use the following standard notation for state-space realizations of a MIMO, linear time-invariant (LTI), noise-free system and its corresponding transfer function

$$G : \begin{cases} \dot{x} = Ax + Bu \\ y = Cx + Du \end{cases} \Leftrightarrow G(s) = \begin{bmatrix} A & B \\ C & D \end{bmatrix}. \quad (1)$$

This will generally be a $p \times q$ system with n states. Going forward, we will assume this system does not have any purely imaginary poles.

A left-tangential barycentric interpolant is a transfer function of the form

$$\begin{aligned} R(s) &:= M^{-1}(s)N(s) := \left(I + \sum_{k=1}^{\ell} \frac{W_k U_k^*}{s - j\omega_k} \right)^{-1} \left(D + \sum_{k=1}^{\ell} \frac{W_k \Sigma_k V_k^*}{s - j\omega_k} \right), \\ &:= ([I \ \mathbb{W}] \mathcal{M}(s))^{-1} [I \ \mathbb{W}] \mathcal{N}(s), \quad (2) \end{aligned}$$

where $W_k \in \mathbb{C}^{p \times r_k}$ are full-column-rank free parameters. The set $\{j\omega_1, \dots, j\omega_\ell\}$ are the interpolation points (on the imaginary axis), and U_k , Σ_k , and V_k form a r_k -rank approximation of $G(j\omega_k) = U_k \Sigma_k V_k^*$ for some pre-specified r_k (obtained from the SVD of $G(j\omega_k)$). Theorem 3.1 [5], [11], [10] below states that for all weight matrices, $R(s)$ above is a *left-interpolant* of $G(s)$ at the points $\{j\omega_k\}$, i.e. $U_k^* G(j\omega_k) = U_k^* R(j\omega_k)$ for each ω_k .

The second line in (2) states that the weights in M and N can be factored out into a matrix

$$\mathbb{W} := [w_1 \ \dots \ w_\ell] \in \mathbb{C}^{p \times r} \quad (3)$$

containing all the weights, and forming two block column systems $\mathcal{M} \in \mathbb{C}^{(p+r) \times p}$ and $\mathcal{N} \in \mathbb{C}^{(p+r) \times q}$, where $r = \sum_{k=1}^{\ell} r_k$. This is detailed in Theorem 3.2 which also shows that R has a state-space representation with state dimension r that can be constructed from matrices consisting only of interpolation data and the matrix of free parameters.

To use the interpolant (2) as a reduced order model, two questions must be answered. First, how should one select the interpolation frequencies and their respective approximation ranks? Additionally, what methods should be used to determine the values of the weight matrices? The algorithm that we have developed is an iterative algorithm loosely based on the AAA algorithm that builds up a model by selecting one new interpolation frequency per iteration, then readjusts the weights by solving an optimization problem which minimizes the error across the frequency spectrum. We will view these steps in more detail in their own sections, but we will begin to address them now, starting with the weight optimization.

Supposing a set of interpolation frequencies has already been selected. We consider a weighted H_2 norm which optimizes the free weight parameters in (2) to minimize the squared error across the frequency spectrum, weighted by M :

$$\min_{\mathbb{W}} \int_0^\infty \|M(j\omega)(R(j\omega) - G(j\omega))\|_F^2 d\omega.$$

Due to the manner in which the weights appear in (2), this optimization problem can be stated as follows.

Problem 1:

$$\min_{\mathbb{W}} \|[I \ \mathbb{W}] \underbrace{(\mathcal{N} - \mathcal{M}G)}_H\|_{H_2}^2.$$

As shown in Theorem 3.3, The system H appearing in Problem 1 has the state space representation

$$H := \mathcal{N} - \mathcal{M}G = \begin{bmatrix} A & B \\ -C & 0 \\ \mathcal{E}_\ell & 0 \end{bmatrix}, \quad \mathcal{E}_\ell = \begin{bmatrix} c_1 \\ \vdots \\ c_\ell \end{bmatrix} \in \mathbb{C}^{r \times n}, \quad (4)$$

where

$$C_k = \begin{cases} U_k^* C(j\omega_k I - A)^{-1} & \text{if } G \text{ complex or } \omega_k = 0 \\ \begin{bmatrix} \Re(U_k^* C(j\omega_k I - A)^{-1}) \\ -\Im(U_k^* C(j\omega_k I - A)^{-1}) \end{bmatrix} & \text{o.w.} \end{cases},$$

thus we are able to recast Problem 1 as the following trace minimization problem.

Problem 2:

$$\min_{\mathbb{W}} \gamma_\ell(\mathbb{W}), \text{ where} \\ \gamma_\ell(\mathbb{W}) := \text{tr} \left([I \ \mathbb{W}] \begin{bmatrix} C\Theta C^* & -C\Theta \mathcal{C}_\ell^* \\ -\mathcal{C}_\ell \Theta C^* & \mathcal{C}_\ell \Theta \mathcal{C}_\ell^* \end{bmatrix} [I \ \mathbb{W}^*] \right)$$

where Θ is the controllability Gramian of the original system. Under mild assumptions, we show in Theorem 4.1 that Problem 2 and thus Problem 1 have explicit formulae for the global minimizer

$$\mathbb{W}_{\ell, \min} = C\Theta \mathcal{C}_\ell^* (\mathcal{C}_\ell \Theta \mathcal{C}_\ell^*)^{-1}$$

for $r \leq n_{\min}$, the size of the minimal realization of the input system. Furthermore, we show that with this choice on \mathbb{W} , the error monotonically decreases across subsequent iterations, i.e. $\gamma_{\ell+1}(\mathbb{W}_{\ell+1, \min}) \leq \gamma_\ell(\mathbb{W}_{\ell, \min})$, and reaches zero once $r \geq n_{\min}$. Importantly, this implies that the H_2 error norm between the input system and the reduced-order system also reaches zero once the reduced-order system's size reaches the size of a minimal realization of the input system.

This weighted norm will decrease across iterations as long as each interpolation frequency is distinct, thus there is freedom in how we choose the next interpolation frequency each iteration. We introduce three methods, with the first being interpolating at the frequency of maximum error, i.e. the frequency at which the L_∞ norm of the error system is attained. In this case, an H_∞ bisection algorithm is used to find the frequency at every step. This is computationally expensive, however, so we introduce two other methods, which we term the gridded and random approaches. The three aforementioned methods form three algorithms that trade off computational complexity, approximation performance, and determinism.

III. STATE SPACE REALIZATIONS

In our prior work, we began investigating what we termed low-rank interpolation [10], which uses a left-tangential interpolant. In this work, we use this interpolant as a basis to derive a left-tangential interpolating system and a variant which has real-valued coefficients. We note that similar descriptor realizations for tangential interpolants appear in Antoulas' work, but a more concrete connection between these descriptor systems and barycentric interpolants first appeared in [11]. Following the derivation of the system representation and its real-valued counterpart, we provide a summary which unifies these two realizations into a common form. We then end the section by finding a state-space realization of $H := \mathcal{N} - \mathcal{M}G$, which is used extensively in the optimization step.

A. Left-tangential interpolating systems

We start by considering a left-tangential barycentric interpolant shown in equation (2), which was introduced at the end of our previous work [10]. We show in Theorem 3.1 that this function satisfies the left-interpolation property of $U_k^* G(j\omega_k) = U_k^* R(j\omega_k)$ and that $G(s)$ tends towards D as s approaches infinity.

Assumption 1: Consider the system G , let $\{\omega_i\}_{i=1}^\ell$ be a set of distinct real numbers, and let $\{r_i\}_{i=1}^\ell$ be a set of ranks. Consider the rank- r_i -truncated SVD of $G(\cdot)$ at each $j\omega_i$ where r_i is less than or equal to the rank of $G(j\omega_i)$, i.e. $U_i \Sigma_i V_i^*$ forms the best rank- r_i approximation of $G(j\omega_i)$. Under these assumptions, we have $U_i \in \mathbb{C}^{p \times r_i}$, $U_i^* U_i = I$, diagonal full-rank $\Sigma_i \in \mathbb{R}^{r_i \times r_i}$, $V_i \in \mathbb{C}^{q \times r_i}$, and $V_i^* V_i = I$.

Theorem 3.1: Consider the assumptions in Assumptions 1 and the interpolant R from equation (2), where each $W_i \in \mathbb{C}^{p \times r_i}$, $i = 1, \dots, \ell$ is a full-column-rank free parameter. Then, R left-interpolates G at each $j\omega_i$ for any valid weight $W_i \in \mathbb{C}^{p \times r_i}$, and $\lim_{|s| \rightarrow \infty} R(s) = D$.

Now, we will provide state-space realizations for the terms appearing equation (2). The system $R(s)$ is the product of two systems M^{-1} , and N . Both M and N contain terms which are left-multiplied by a weight, thus they may each be written as a product between the weight matrix \mathbb{W} and a block-column system, i.e. $M = [I \ \mathbb{W}] \mathcal{M}$ and $N = [I \ \mathbb{W}] \mathcal{N}$, where $\mathbb{W} = [w_1 \ \dots \ w_\ell] = [I \ \mathbb{W}]$,

$$\mathcal{M}(s) := \begin{bmatrix} \mathcal{M}_1(s) \\ \vdots \\ \mathcal{M}_\ell(s) \end{bmatrix}, \text{ and } \mathcal{N}(s) := \begin{bmatrix} \mathcal{N}_1(s) \\ \vdots \\ \mathcal{N}_\ell(s) \end{bmatrix}.$$

Each sub-system in \mathcal{M} and \mathcal{N} ,

$$\mathcal{M}_k := \frac{U_k^*}{s - j\omega_k}, \text{ and } \mathcal{N}_k := \frac{\Sigma_k V_k^*}{s - j\omega_k},$$

have readily apparent state-space realizations, namely

$$\mathcal{M}_k = \left[\begin{array}{c|c} j\omega_k I & U_k^* \\ \hline I & 0 \end{array} \right], \mathcal{N}_k = \left[\begin{array}{c|c} j\omega_k I & \Sigma_k V_k^* \\ \hline I & 0 \end{array} \right]. \quad (5)$$

State-space realizations for \mathcal{M} , \mathcal{N} , M , and N can now be constructed by concatenating each of these systems. Indeed,

$$\mathcal{M} = \left[\begin{array}{c|c} \mathcal{A} & \mathcal{B}_m \\ \hline 0 & I \\ \hline I & 0 \end{array} \right], \quad \mathcal{N} = \left[\begin{array}{c|c} \mathcal{A} & \mathcal{B}_n \\ \hline 0 & D \\ \hline I & 0 \end{array} \right], \quad (6)$$

$$M = \left[\begin{array}{c|c} \mathcal{A} & \mathcal{B}_m \\ \hline \mathbb{W} & I \end{array} \right], \quad N = \left[\begin{array}{c|c} \mathcal{A} & \mathcal{B}_n \\ \hline \mathbb{W} & D \end{array} \right]. \quad (7)$$

where

$$\mathcal{A} := \text{diag}(j\omega_1 I, \dots, j\omega_\ell I), \quad [\mathcal{B}_M \ \mathcal{B}_N] := \begin{bmatrix} U_1^* \Sigma_1 V_1^* \\ \vdots \\ U_\ell^* \Sigma_\ell V_\ell^* \end{bmatrix}$$

are matrices that consist only of interpolation data. From these realizations, it is possible to find a realization of R as shown in Theorem 3.2. The realizations of M and N have poles on the imaginary axis, but due to pole-zero cancellations in R , we show that the realization of R does not. Importantly, this shows it is possible to form a state-space realization of the system by forming three matrices from interpolation data (\mathcal{A} , \mathcal{B}_M , and \mathcal{B}_N) and one matrix \mathbb{W} from the free parameters.

Theorem 3.2: Let M and N be defined as in equation (7) and let $R = M^{-1}N$. Then,

$$R = \left[\begin{array}{c|c} \frac{\mathcal{A} - \mathcal{B}_M \mathbb{W}}{\mathbb{W}} & \frac{\mathcal{B}_N - \mathcal{B}_M D}{D} \\ \hline & \end{array} \right]. \quad (8)$$

Proof: Because M has an invertible feedthrough matrix, we can find a state space representation for M^{-1} , which is

$$M^{-1} = \left[\begin{array}{c|c} \frac{\mathcal{A} - \mathcal{B}_M \mathbb{W}}{-\mathbb{W}} & \frac{\mathcal{B}_M}{I} \\ \hline & \end{array} \right].$$

Thus we can find a combined state space realization for R by cascading the realizations for M^{-1} and N , giving

$$R = \left[\begin{array}{cc|c} \mathcal{A} & 0 & \mathcal{B}_N \\ \mathcal{B}_M \mathbb{W} & \mathcal{A} - \mathcal{B}_M \mathbb{W} & \mathcal{B}_M D \\ \hline \mathbb{W} & -\mathbb{W} & D \end{array} \right].$$

Performing a coordinate change with the transformation matrix $\frac{1}{2} \begin{bmatrix} I & I \\ -I & I \end{bmatrix}$ yields

$$R = \left[\begin{array}{cc|c} \mathcal{A} - \mathcal{B}_M \mathbb{W} & 0 & \mathcal{B}_N - \mathcal{B}_M D \\ \mathcal{B}_M \mathbb{W} & \mathcal{A} & \mathcal{B}_N + \mathcal{B}_M D \\ \hline \mathbb{W} & 0 & D \end{array} \right].$$

From this it is clear that the second block mode is unobservable and can be eliminated, yielding equation (8). ■

B. Enforcing real coefficients

In the case that G has real coefficients, we see the realization of R shown in equation (8) will not have real coefficients in general due to the presence of complex values in \mathcal{A} , \mathcal{B}_M , and \mathcal{B}_N . Thus, we will consider an interpolation strategy that guarantees a realization of R with real coefficients exists. The strategy we consider is, when interpolating at a non-zero frequency ω , to interpolate at both $j\omega$ and $-j\omega$. We lay out an argument for why we consider this, and show that with this strategy, there is a specific choice of weights which yields a resulting system with real coefficients.

When G has real coefficients, it is the case that $\overline{G}(j\omega) = G(-j\omega)$ for all $\omega \in \mathbb{R}$ that isn't a pole of G . Similarly, supposing R has real coefficients, then it must be the case that $\overline{R}(j\omega) = R(-j\omega)$ for all $\omega \in \mathbb{R}$. Consider interpolating at a point $j\omega_k$ ensuring $U_k^* G(j\omega_k) = \Sigma_k V_k^* = U_k^* R(j\omega_k)$. Under the assumption that R has real coefficients, it follows that

$$\overline{U}_k^* G(-j\omega_k) = \Sigma_k \overline{V}_k^* = \overline{U}_k^* R(-j\omega_k),$$

which implies that, when G and R have real coefficients, there is an additional interpolation constraint that is always satisfied for $-j\omega_k$. Going forward, we will thus consider interpolating at both $j\omega_k$ and $-j\omega_k$ when $\omega_k > 0$ and check conditions on the weights to ensure realness. Importantly, when $j\omega_k = 0$, $G(0)$ and thus the corresponding data in \mathcal{A} , \mathcal{B}_M , and \mathcal{B}_N are real, implying we only need to consider the case where $\omega_k > 0$.

Consider the pair of terms in $M(s)$ resulting in interpolating at $\pm j\omega_k$ where $\omega_k > 0$, which could be written as

$$\begin{aligned} & \frac{W_{k,1} U_k^*}{s - j\omega_k} + \frac{W_{k,2} \overline{U}_k^*}{s + j\omega_k} = \\ & \frac{(W_{k,1} U_k^* + W_{k,2} \overline{U}_k^*)s + (W_{k,1} U_k^* - W_{k,2} \overline{U}_k^*)j\omega_k}{s^2 + \omega_k^2}. \end{aligned}$$

We require the coefficients in the numerator to be real independent of the values of U_k and ω_k , implying $\Im(W_{k,1} U_k^* + W_{k,2} \overline{U}_k^*) = 0$ and $\Re(W_{k,1} U_k^* - W_{k,2} \overline{U}_k^*) = 0$. It turns out the only relation that satisfies these requirements is $W_{k,1} = \overline{W}_{k,2}$. With this in mind, the pair can now be written as

$$\frac{2s \Re(W_{k,1} U_k^*) - 2\omega_k \Im(W_{k,1} U_k^*)}{s^2 + \omega_k^2}.$$

Now we expand out both terms and factor out $\Re(W_{k,1})$ and $\Im(W_{k,1})$ from the expression, which forms the matrix $W_k := 2[\Re(W_{k,1}) \ \Im(W_{k,1})]$, which is a real-valued free parameter. We are left with

$$\mathcal{M}_k(s) := \frac{\begin{bmatrix} \Re(U_k^T) s + \Im(U_k^T) \omega_k \\ \Im(U_k^T) s - \Re(U_k^T) \omega_k \end{bmatrix}}{s^2 + \omega_k^2}$$

Following the same procedure, the pairs of terms in $N(s)$ for $\omega > 0$ can be combined which produces

$$\mathcal{N}_k(s) := \frac{\begin{bmatrix} \Sigma_k \Re(V_k^T) s + \Sigma_k \Im(V_k^T) \omega_k \\ \Sigma_k \Im(V_k^T) s - \Sigma_k \Re(V_k^T) \omega_k \end{bmatrix}}{s^2 + \omega_k^2}.$$

These systems have the realizations

$$\mathcal{M}_k = \left[\begin{array}{cc|c} 0 & \omega_k I & \Re(U_k^T) \\ -\omega_k I & 0 & \Im(U_k^T) \\ \hline I & 0 & 0 \\ 0 & I & 0 \end{array} \right], \text{ and} \quad (9)$$

$$\mathcal{N}_k = \left[\begin{array}{cc|c} 0 & \omega_k I & \Sigma_k \Re(V_k^T) \\ -\omega_k I & 0 & \Sigma_k \Im(V_k^T) \\ \hline I & 0 & 0 \\ 0 & I & 0 \end{array} \right]. \quad (10)$$

Remark 3.1: As an aside, let the systems \mathcal{M}_k and \mathcal{N}_k from equation (5) be \mathcal{M}_k^c and \mathcal{N}_k^c respectively. The systems \mathcal{M}_k and \mathcal{N}_k from equations (9) and (10) can be written as

$$\mathcal{M}_k = \begin{bmatrix} \Re(\mathcal{M}_k^c) \\ -\Im(\mathcal{M}_k^c) \end{bmatrix} \text{ and } \mathcal{N}_k = \begin{bmatrix} \Re(\mathcal{N}_k^c) \\ -\Im(\mathcal{N}_k^c) \end{bmatrix}$$

respectively. We denote $\Re(G)$ and $\Im(G)$ to be the systems defined by $\Re(G) = \frac{1}{2}(G + \overline{G})$ and $\Im(G) = \frac{1}{2j}(G - \overline{G})$. State space representations exist for these systems, namely

$$\begin{bmatrix} \Re(G) \\ \Im(G) \end{bmatrix} = \left[\begin{array}{cc|c} \Re(A) & -\Im(A) & \Re(B) \\ \Im(A) & \Re(A) & \Im(B) \\ \hline \Re(C) & -\Im(C) & \Re(D) \\ \Im(C) & \Re(C) & \Im(D) \end{array} \right].$$

Thus, in the case that G has real coefficients, we see we can interpolate at both $j\omega_k$ and $-j\omega_k$ when $\omega_k > 0$ and choose the resulting weights to guarantee that \mathcal{M}_k and \mathcal{N}_k have a realization with real coefficients. In the case that $\omega_k = 0$, those realizations are already real. Thus, assuming \mathbb{W} is also real, it is also the case that R is real. We now make an important observation. These new \mathcal{M}_k and \mathcal{N}_k systems are functionally the same as the ones seen in equation (5): they are left-multiplied by a free-parameter weight, then summed to form M and N . The difference is in the form of the A and B matrices. Thus, we can succinctly describe both situations as shown below.

Given a system G , a set of frequencies $\{\omega_k\}_{k=1}^\ell$ each of which is a real number and non-negative if G has real coefficients, and a set of integer approximation ranks $\{r_k\}_{k=1}^\ell$ which

are between 1 and p , we can construct a (real) left-tangential interpolating system by considering the results stated above. First, for each frequency ω_k , we find the corresponding response $G(j\omega_k)$ and let $U_k \Sigma_k V_k^*$ be its best r_k approximation constructed from the SVD, ensuring r_k does not exceed the rank of $G(j\omega_k)$. Now, from equations (5), (9), and (10), we let

$$[\mathcal{M}_k \ \mathcal{N}_k] = \left[\begin{array}{c|cc} \mathcal{A} & \mathcal{B}_{M,k} & \mathcal{B}_{N,k} \\ \hline I & 0 & 0 \end{array} \right], \text{ where} \quad (11)$$

$$\mathcal{A}_k = \begin{cases} j\omega_k I & \text{if } \omega_k = 0 \text{ or } G \text{ complex} \\ \begin{bmatrix} 0 & \omega_k I \\ -\omega_k I & 0 \end{bmatrix} & \text{o.w.} \end{cases} \quad (12)$$

$$[\mathcal{B}_{M,k} \ \mathcal{B}_{N,k}] = \begin{cases} [U_k^* \ \Sigma_k V_k^*] & \text{if } \omega_k = 0 \text{ or } G \text{ complex} \\ \begin{bmatrix} \Re(U_k^T) & \Sigma_k \Re(V_k^T) \\ \Im(U_k^T) & \Sigma_k \Im(V_k^T) \end{bmatrix} & \text{o.w.} \end{cases} \quad (13)$$

We redefine the following matrices

$$\mathcal{A} := \begin{bmatrix} \mathcal{A}_1 & & \\ & \ddots & \\ & & \mathcal{A}_\ell \end{bmatrix}, \quad [\mathcal{B}_M \ \mathcal{B}_N] := \begin{bmatrix} \mathcal{B}_{M,1} & \mathcal{B}_{N,1} \\ \vdots & \vdots \\ \mathcal{B}_{M,\ell} & \mathcal{B}_{N,\ell} \end{bmatrix},$$

and note that state-space realizations for \mathcal{M} , \mathcal{N} , M , N , and R are given in equations (6), (7), and (8) respectively. In terms of sizes, we note that the number of states n_k of \mathcal{M}_k or \mathcal{N}_k is r_k if $\omega_k = 0$ or if G has complex coefficients, or $2r_k$ otherwise. We will call the sum of these states r , thus all of \mathcal{M} , \mathcal{N} , M , N , and R have r states. Additionally, we note $\mathcal{M}(s) \in \mathbb{C}^{p+r \times p}$, $\mathcal{N}(s) \in \mathbb{C}^{p+r \times q}$, and $\mathbb{W} \in \mathbb{C}^{p \times r}$.

C. The system H

The system $H := \mathcal{N} - \mathcal{M}G$ appears in Problem 1, and we show in the next section the well-posedness depends on the properties of this system. Here, we show that H admits a very nice representation in that its A and B matrices are identical to that of the input system.

Theorem 3.3: Suppose $H = \mathcal{N} - \mathcal{M}G$, where

$$\mathcal{M} = \begin{bmatrix} M_1(s) \\ \vdots \\ M_\ell(s) \end{bmatrix}, \quad \mathcal{N} = \begin{bmatrix} N_1(s) \\ \vdots \\ N_\ell(s) \end{bmatrix}, \text{ and}$$

$$[\mathcal{M}_k \ \mathcal{N}_k] = \begin{cases} \left[\begin{array}{c|cc} j\omega_k I & U_k^* & \Sigma_k V_k^* \\ \hline I & 0 & 0 \end{array} \right] & \text{if } G \text{ complex or } \omega_k = 0 \\ \left[\begin{array}{ccc|cc} 0 & \omega_k I & \Re(U_k^T) & \Sigma_k \Re(V_k^T) \\ -\omega_k I & 0 & \Im(U_k^T) & \Sigma_k \Im(V_k^T) \\ \hline I & 0 & 0 & 0 \\ 0 & I & 0 & 0 \end{array} \right] & \text{o.w.} \end{cases}$$

Then the system H has the realization

$$H = \left[\begin{array}{c|c} A & B \\ \hline -C & 0 \\ \mathcal{C}_\ell & 0 \end{array} \right], \quad \mathcal{C}_\ell = \begin{bmatrix} C_1 \\ \vdots \\ C_\ell \end{bmatrix} \in \mathbb{C}^{r \times n}, \quad (14)$$

and

$$C_k = \begin{cases} U_k^* C(j\omega_k I - A)^{-1} & \text{if } G \text{ complex or } \omega_k = 0 \\ \begin{bmatrix} \Re(U_k^* C(j\omega_k I - A)^{-1}) \\ -\Im(U_k^* C(j\omega_k I - A)^{-1}) \end{bmatrix} & \text{o.w.} \end{cases}$$

IV. WEIGHT OPTIMIZATION

Using the interpolating systems that were introduced in the previous section, we now turn to the optimization step of the algorithm, in which we assume a valid set of interpolation points has been chosen and we optimize a proxy for the error over all frequencies. Here we derive an explicit solution for the weights that minimize a weighted H_2 norm of the error system. We also provide bounds on said H_2 norm and show convergence to the input system when the number of states reaches the number of jointly observable and controllable states in the input system.

Because adjusting the weights affects the frequency response across the frequency spectrum, careful selection of the weights can be used to decrease the approximation. We would like to choose the weights \mathbb{W} to minimize the mean squared error between R and G , and ideally, we would try to optimize the H_2 norm of $R - G$, supposing both systems are stable. This is a difficult problem due to the appearance of \mathbb{W} in both M^{-1} and N , however, so instead we will focus on choosing \mathbb{W} such that it solves the weighted H_2 minimization

$$\begin{aligned} \min_{\mathbb{W}} \|M[\mathbb{W}](R[\mathbb{W}] - G)\|_{H_2}^2 &= \min_{\mathbb{W}} \|N[\mathbb{W}] - M[\mathbb{W}]G\|_{H_2}^2 \\ &= \min_{\mathbb{W}} \|[I \ \mathbb{W}](\underbrace{\mathcal{N} - \mathcal{M}G}_H)\|_{H_2}^2, \end{aligned}$$

i.e. Problem 1. We later argue through computational examples that solving this optimization problem instead yields a system which still approximates the original system well in the H_2 sense. With some algebra, we see that this problem is equivalent to

$$\begin{aligned} \min_{\mathbb{W}} \int_0^\infty \text{tr}([I \ \mathbb{w}]H(j\omega)H^*(j\omega)\begin{bmatrix} I \\ \mathbb{w}^* \end{bmatrix}) d\omega \\ = \min_{\mathbb{W}} \text{tr}([I \ \mathbb{W}]X\begin{bmatrix} I \\ \mathbb{W}^* \end{bmatrix}), \end{aligned}$$

where

$$X = \int_0^\infty H(j\omega)H^*(j\omega)d\omega. \quad (15)$$

For X to exist, H must have a zero feedthrough and H must not have any poles on the imaginary axis. As shown in the previous section in Theorem 3.3, we see that H has a realization with zero feedthrough and has an A matrix which is identical to the A matrix of the input system G . Since we assume G has no poles on the imaginary axis, X exists, and a closed form for it can be constructed using controllability Gramian of the system G . Expanding $H(j\omega)$ with the new realization of H in equation (19), we get

$$\begin{aligned} X &= \int_0^\infty \begin{bmatrix} -C \\ \mathcal{C}_\ell \end{bmatrix} (j\omega I - A)^{-1} B B^* (j\omega I - A)^{-*} \begin{bmatrix} -C \\ \mathcal{C}_\ell \end{bmatrix}^* d\omega \\ &= \begin{bmatrix} -C \\ \mathcal{C}_\ell \end{bmatrix} \left(\int_0^\infty \theta(j\omega)\theta^*(j\omega)d\omega \right) \begin{bmatrix} -C^* \\ \mathcal{C}_\ell^* \end{bmatrix}, \end{aligned}$$

where $\theta(s) = (sI - A)^{-1}B$. This integral equals the controllability Gramian of G , which we will denote Θ . Therefore

$$X = \begin{bmatrix} C\Theta C^* & -C\Theta\mathcal{C}_\ell^* \\ -\mathcal{C}_\ell\Theta C^* & \mathcal{C}_\ell\Theta\mathcal{C}_\ell^* \end{bmatrix},$$

and our minimization problem becomes

$$\min_{\mathbb{W}} \gamma_\ell(\mathbb{W}), \text{ where} \quad (16)$$

$$\gamma_\ell(\mathbb{W}) = \text{tr} \left([I \ \mathbb{W}] \begin{bmatrix} C\Theta C^* & -C\Theta\mathcal{C}_\ell^* \\ -\mathcal{C}_\ell\Theta C^* & \mathcal{C}_\ell\Theta\mathcal{C}_\ell^* \end{bmatrix} \begin{bmatrix} I \\ \mathbb{W}^* \end{bmatrix} \right),$$

which we have previously denoted Problem 2. According to Theorem 4.1, under mild assumptions, this problem always has a solution which is unique as long as the number of interpolation points is less than or equal to the number of jointly controllable and observable modes in G .

Theorem 4.1: Consider the minimization in Problem 2, and let n_{\min} be the size of a minimal realization of G . If $r \leq n_{\min}$, then the unique solution for \mathbb{W} is

$$\mathbb{W} = C\Theta\mathcal{C}_\ell^* (\mathcal{C}_\ell\Theta\mathcal{C}_\ell^*)^{-1},$$

with \mathcal{C}_ℓ defined as in equation (19). If $r > n_{\min}$, partition \mathcal{C}_ℓ into $\begin{bmatrix} \widehat{\mathcal{C}}_\ell \\ \widetilde{\mathcal{C}}_\ell \end{bmatrix}$ where $\widehat{\mathcal{C}}_\ell \in \mathbb{C}^{n_{\min} \times n}$, and define $P \in \mathbb{C}^{r-n_{\min} \times n_{\min}}$ such that $\widetilde{\mathcal{C}}_\ell = P\widehat{\mathcal{C}}_\ell$. Then the minimizer is

$$\mathbb{W} = \begin{bmatrix} C\Theta\widehat{\mathcal{C}}_\ell^* (\widehat{\mathcal{C}}_\ell\Theta\widehat{\mathcal{C}}_\ell^*)^{-1} + FP & -F \end{bmatrix}$$

for some free parameter $F \in \mathbb{C}^{p \times r-n_{\min}}$.

Proof: Expand $\gamma_\ell(\mathbb{W})$ to get

$$\gamma_\ell(\mathbb{W}) = \mathbb{W}\mathcal{C}_\ell\Theta\mathcal{C}_\ell^*\mathbb{W}^* - \mathbb{W}\mathcal{C}_\ell\Theta C^* - C\Theta\mathcal{C}_\ell^*\mathbb{W}^* + C\Theta C^*.$$

Now, we the Gateaux derivative of γ_ℓ , which yields

$$\begin{aligned} \partial_{\mathbb{W}}\gamma_\ell(V) &= \left. \frac{d}{d\delta} \gamma_\ell(\mathbb{W} + \delta V) \right|_{\delta=0} \\ &= \text{tr}(V\mathcal{C}_\ell\Theta\mathcal{C}_\ell^*\mathbb{W}^* + \mathbb{W}\mathcal{C}_\ell\Theta\mathcal{C}_\ell^*V^* \\ &\quad - V\mathcal{C}_\ell\Theta C^* - C\Theta\mathcal{C}_\ell^*V^*). \\ &= 2 \text{tr}(\mathbb{W}\mathcal{C}_\ell\Theta\mathcal{C}_\ell^*V^* - C\Theta\mathcal{C}_\ell^*V^*). \end{aligned}$$

The stationary points of the minimization occur when $\partial_{\mathbb{W}}\gamma_\ell(V) = 0$ for all V , thus the solutions of the optimization must satisfy

$$\begin{aligned} \text{tr}(\mathbb{W}\mathcal{C}_\ell\Theta\mathcal{C}_\ell^*V^* - C\Theta\mathcal{C}_\ell^*V^*) &= 0 \\ \implies \mathbb{W}\mathcal{C}_\ell\Theta\mathcal{C}_\ell^* &= C\Theta\mathcal{C}_\ell^*. \end{aligned} \quad (17)$$

Utilizing the results from Corollary 1.1, we make the substitutions of $\mathcal{C}_\ell\Theta\mathcal{C}_\ell^* = \mathcal{C}_{\ell,\min}\Theta_{\min}\mathcal{C}_{\ell,\min}^*$ and $C\Theta\mathcal{C}_\ell^* = C_{\min}\Theta_{\min}C_{\min}^*$, where the min subscript denotes the use of a minimal realization of G , meaning $\Theta_{\min} > 0$. Also from Corollary 1.1, when $r \leq n_{\min}$, $\mathcal{C}_{\ell,\min}$ is full row rank, thus $\mathcal{C}_{\ell,\min}\Theta_{\min}\mathcal{C}_{\ell,\min}^* > 0$ and $\mathcal{C}_\ell\Theta\mathcal{C}_\ell^*$ is invertible. This implies \mathbb{W} has a unique solution, namely

$$\mathbb{W} = C\Theta\mathcal{C}_\ell^* (\mathcal{C}_\ell\Theta\mathcal{C}_\ell^*)^{-1}.$$

When $r \geq n_{\min}$, we first partition \mathbb{W} and \mathcal{C}_ℓ into $\begin{bmatrix} \widehat{\mathbb{W}} & \widetilde{\mathbb{W}} \end{bmatrix}$ and $\begin{bmatrix} \widehat{\mathcal{C}}_\ell \\ \widetilde{\mathcal{C}}_\ell \end{bmatrix}$ respectively, where $\widehat{\mathbb{W}} \in \mathbb{C}^{p \times n_{\min}}$ and $\widehat{\mathcal{C}}_\ell \in \mathbb{C}^{n_{\min} \times n}$. The rows of $\widetilde{\mathcal{C}}_\ell$ are linearly dependent with the rows of $\widehat{\mathcal{C}}_\ell$ according to Corollary 1.1, thus we can factor $\widetilde{\mathcal{C}}_\ell$ out to get $\mathcal{C}_\ell = \begin{bmatrix} I \\ P \end{bmatrix} \widehat{\mathcal{C}}_\ell$ for some matrix P . Substituting this back into equation (17), we get

$$\begin{aligned} \begin{bmatrix} \widehat{\mathbb{W}} & \widetilde{\mathbb{W}} \end{bmatrix} \begin{bmatrix} I \\ P \end{bmatrix} \widehat{\mathcal{C}}_\ell \Theta \widehat{\mathcal{C}}_\ell^* \begin{bmatrix} I \\ P^* \end{bmatrix} &= C\Theta\widehat{\mathcal{C}}_\ell^* \begin{bmatrix} I \\ P^* \end{bmatrix} \\ (\widehat{\mathbb{W}} + \widetilde{\mathbb{W}}P) \widehat{\mathcal{C}}_\ell \Theta \widehat{\mathcal{C}}_\ell^* &= C\Theta\widehat{\mathcal{C}}_\ell^*. \end{aligned}$$

Thus,

$$\widehat{\mathbb{W}} = C\Theta\widehat{\mathcal{C}}_\ell^* (\widehat{\mathcal{C}}_\ell\Theta\widehat{\mathcal{C}}_\ell^*)^{-1} - \widetilde{\mathbb{W}}P$$

where $\widetilde{\mathbb{W}}$ is now a free parameter, which is re-labeled F in the theorem statement. ■

Now that we have closed form solutions to the optimization problem, we want to understand how the performance of the algorithm across iterations is determined by this choice on \mathbb{W} . Suppose both R and G are stable systems. The optimization problem minimizes the H_2 norm of $N-MG$, which is equal to $\gamma_\ell(\mathbb{W}_{\ell,\min})$ at iteration ℓ . Thus, understanding how γ behaves across iterations gives insight to the overall performance of the algorithm. Theorem 4.2 answers a few of these questions. We see that γ is bounded above by

$$\left\| \begin{bmatrix} A & B \\ C & 0 \end{bmatrix} \right\|_{H_2}$$

and that it is monotonically decreasing across iterations until its size equals the number of jointly controllable and observable modes of the original system, in which case γ is zero. We show then that $R = G$ (up to coordinate changes). We have observed in our numerical examples that the true approximation error, $\|R - G\|_{H_2}$, on average decreases at the same rate, suggesting that there may be an inequality relating these two norms.

Theorem 4.2: Consider the stable system $G = \begin{bmatrix} A & B \\ C & D \end{bmatrix}$ and let \mathbb{W}_ℓ^+ be the minimizer of γ_ℓ at iteration ℓ from Problem 2, which has a closed form solution as described in Theorem 4.1. Let $\gamma_\ell^+ := \gamma_\ell(\mathbb{W}_\ell^+)$. Then, for $\ell \geq 0$,

$$\gamma_{\ell+1}^+ \leq \gamma_\ell^+.$$

Additionally, for $\ell = 0$, $\gamma_0^+ = \left\| \begin{bmatrix} A & B \\ C & 0 \end{bmatrix} \right\|_{H_2}^2$, and when r , the number of poles of R , is equal to or larger than the size of a minimal realization of G , $\gamma_\ell^+ = 0$.

Proof: When $\ell = 0$, \mathcal{C}_ℓ is an empty $0 \times n$ matrix, and γ_0^+ simplifies to $\gamma_0^+ = \text{tr}(C\Theta C^*)$, which by definition is the square of the H_2 norm of the system $\begin{bmatrix} A & B \\ C & 0 \end{bmatrix}$.

From Theorem 4.1, for $r \leq n_{\min}$, the unique solution to the minimization problem is

$$\mathbb{W}_\ell^+ = C\Theta\mathcal{C}_\ell^* (\mathcal{C}_\ell\Theta\mathcal{C}_\ell^*)^{-1},$$

and for $r > n_{\min}$, a minimizer is

$$\mathbb{W}_\ell^+ = [C\Theta\widehat{\mathcal{C}}_\ell^* (\widehat{\mathcal{C}}_\ell\Theta\widehat{\mathcal{C}}_\ell^*)^{-1} \ 0].$$

Due to Lemma 1.1, we make the substitutions $C\Theta C^* = C_{\min}\Theta_{\min}C_{\min}^*$, $C\Theta\mathcal{C}_\ell^* = C_{\min}\Theta_{\min}\mathcal{C}_{\ell,\min}^*$, and $\mathcal{C}_\ell\Theta\mathcal{C}_\ell^* = \mathcal{C}_{\ell,\min}\Theta_{\min}\mathcal{C}_{\ell,\min}^*$ into \mathbb{W}_ℓ^+ and γ_ℓ^+ . We note that $\widehat{\mathcal{C}}_\ell \in \mathbb{C}^{n_{\min} \times n_{\min}}$ and Θ_{\min} are invertible, thus the simplification of \mathbb{W}_ℓ^+ simplifies to $[C\widehat{\mathcal{C}}_\ell \Theta_{\min}^{-1} \ 0]$. Substituting this into γ_ℓ and expanding gives $\gamma_\ell^+ = 0$.

Now let $\mathcal{C}_{\ell+1} = \begin{bmatrix} \mathcal{C}_\ell \\ \end{bmatrix}$ and consider the solution that minimizes $\gamma_{\ell+1}(\cdot)$, which is $\mathbb{W}_{\ell+1}^+$. When evaluating the suboptimal quantity $\gamma_{\ell+1}(\mathbb{W}_\ell^+)$, we get

$$\gamma_{\ell+1}(\mathbb{W}_\ell^+) = \text{tr} \left(\begin{bmatrix} I \\ \mathbb{W}_\ell^+ \end{bmatrix} \begin{bmatrix} C\Theta C^* & -C\Theta\mathcal{C}_{\ell+1}^* \\ -\mathcal{C}_{\ell+1}\Theta C^* & \mathcal{C}_{\ell+1}\Theta\mathcal{C}_{\ell+1}^* \end{bmatrix} \begin{bmatrix} I \\ \mathbb{W}_\ell^{+*} \end{bmatrix} \right)$$

which exactly equals γ_ℓ^+ . Because this is a suboptimal solution, we know $\gamma_{\ell+1}^+ \leq \gamma_{\ell+1}(\mathbb{W}_\ell^+)$, thus $\gamma_{\ell+1}^+ \leq \gamma_\ell^+$. ■

Corollary 4.1: When $r = n_{\min}$, $\|R - G\|_{H_2} = 0$, thus $R = G$.

Proof: Previously we showed $\|M(R - G)\|_{H_2}^2 = \gamma_{\ell, \min}$. Thus when $r = n_{\min}$, $\|M(R - G)\|_{H_2} = 0$. Because

$$\|R - G\|_{H_2} \leq \sqrt{p} \|M^{-1}\|_{H_\infty} \|M(R - G)\|_{H_2},$$

it follows that $\|R - G\| \leq 0$, implying $R - G = 0$, or $R = G$ (i.e. there exists a similarity transform between their minimal realizations). ■

To summarize, we see that choosing the weight matrix \mathbb{W} via an optimization on the weighted norm $\|N - MG\|_{H_2}$ admits an explicit solution that has a simple form and is computationally efficient to compute. We also show that the weighted norm is monotonically decreasing as the number of iterations increase, and once R is as large as a minimal realization of G , it is equal to G up to coordinate changes.

V. INTERPOLATION POINTS SELECTION

The previous two sections laid out the theoretical results for the work we present in this paper. In this section, we explore various strategies of selecting the interpolating frequencies as well as the approximation rank at said frequencies. In the first subsection, we first introduce a strategy inspired by the AAA algorithm and interpolate at the frequency where the error is largest. Following that, we consider a random strategy and a grid strategy, both of which are computationally simpler. We also lay out some important considerations in terms of choosing the rank of the approximation for each candidate frequency we select. We end the section by summarizing the algorithm as a whole and provide pseudocode detailing the implementation.

A. Frequency selection strategies

In each iteration of the AAA algorithm, the next interpolation point is chosen to the point which has the largest approximation error from the large set of test points [6]. Intuitively, interpolating where the error is maximized should improve the approximation at that point and nearby points and lower the total error more than any other choice. Thus, interpolating at the frequency where the spectral norm of the error system $R - G$ is maximized is a reasonable choice for our algorithm. In other words, at the ℓ th iteration, we select ω_ℓ to be

$$\omega_\ell = \arg \max_{\omega \in \mathbb{R}} \|R(j\omega) - G(j\omega)\|_2. \quad (18)$$

This frequency occurs where the peak gain is attained for the system $R - G$, thus a H_∞ bisection search may be used to calculate where the next interpolation point will be. These methods are already widely available, such as in MATLAB, where one can use the `getPeakGain` function, which uses a variant of the algorithm in [12]. This algorithm converges in a small number of steps, but at each of those steps, all eigenvalues of a Hamiltonian matrix with size $2(r + n)$ must be computed, which can be quite slow for large systems computationally speaking; when $r \ll n$, this step would have a computational complexity of $O(n^3)$.

Algorithm 1 Maximum error frequency selection

Require: G, R

1: **return** frequency returned from `getPeakGain`($G - R$)

1) *Random and discrete strategies:* Unfortunately, this may be unacceptably slow for large systems, thus we consider two alternative approaches that sidestep this computational bottleneck. The first strategy is a discrete approach where we are given a set of frequencies $\{\hat{\omega}_k\}_{k=1}^K$ and choose the interpolation point from this set where the error is highest, i.e. the maximum value of $\|R(j\hat{\omega}_k) - G(j\hat{\omega}_k)\|_2$ among all $\hat{\omega}_k$. Assuming a zero-pole-gain input model is available and $r \ll n$, this operation may be done in $O(Kn)$. The performance of this method may depend on how fine the grid is, so K may have to be very large to get good performance.

Algorithm 2 Discrete frequency selection

Require: $G, R, \{\hat{\omega}_k\}_{k=1}^K$

1: **return** the $\hat{\omega}_k$ that maximizes $\|R(j\hat{\omega}_k) - G(j\hat{\omega}_k)\|_2$

We will consider an additional strategy of choosing the frequency stochastically. First, we pick K random frequencies $\{\hat{\omega}_k\}_{k=1}^K$ logarithmically between ω_{\min} and ω_{\max} . Then, we calculate the error norm for each frequency and let ω_ℓ be the frequency that maximizes the norm. Like the previous method, this operation may be done in $O(Kn)$.

Algorithm 3 Random frequency selection

Require: $\omega_{\min}, \omega_{\max}, R, G, K$

1: $\{\hat{\omega}_k\}_{k=1}^K \leftarrow K$ log-randomly distributed numbers in $[\omega_{\min}, \omega_{\max}]$

2: **return** the $\hat{\omega}_k$ that maximizes $\|R(j\hat{\omega}_k) - G(j\hat{\omega}_k)\|_2$

B. Rank considerations

The final consideration is the method of choosing the rank of interpolation at each frequency. In most cases, interpolating the singular vector corresponding to the largest singular value is acceptable. However, if the next largest singular values at that frequency are very close in magnitude, interpolating all of them may be worth consideration. We can then define a ‘‘cut-off’’ value $0 < \rho \leq 1$ and include all singular vectors that correspond to singular values larger than ρ times the largest singular value.

In the case that the candidate frequency is close to an already-interpolated frequency, we may instead increase the rank of the existing frequency by incorporating the next largest singular vector. After calculating a candidate frequency ω_ℓ , consider the closest existing interpolation frequency $\bar{\omega}$. If the relative difference $|(\omega_\ell - \bar{\omega})/\omega_\ell|$ is less than some threshold value μ , then we may increase the approximation rank of $\bar{\omega}$ instead of adding a new interpolation point. The implementation of these two ideas are shown in Algorithm 4.

Algorithm 4 Frequency and rank refinement

Require: G , m , $\{\omega_k\}_{k=1}^m$, $\{r_k\}_{k=1}^m$, ω , μ , ρ

- 1: $r_{\min}, \text{new} \leftarrow 1, \text{true}$
- 2: **if** $m > 0$ **then**
- 3: $i \leftarrow$ index of nearest freq. in $\{\omega_k\}_{k=1}^m$ to ω
- 4: **if** $\omega_i = \omega = 0$ or $|(\omega_i - \omega)/\omega| < \mu$ **then**
- 5: $\omega, r_{\min}, \text{new} \leftarrow \omega_i, r_i + 1, \text{false}$
- 6: $\sigma \leftarrow r_{\min}$ th largest singular value of $G(j\omega)$
- 7: $r_{\max} \leftarrow$ index of smallest S.V. $\geq \rho\sigma$
- 8: **if new then**
- 9: $m \leftarrow m + 1$
- 10: $\omega_m, r_m \leftarrow \omega, r_{\max}$
- 11: **else**
- 12: $r_i \leftarrow r_{\max}$
- 13: **return** $\omega, r_{\min}, r_{\max}$

C. Summary

Algorithm 5 provides an overview of the algorithm. First, various variables are initialized and the controllability Gramian of the input system is calculated. Then, one of the previous frequency selection methods is used to find a candidate frequency, which is then used in the rank refinement step. A SVD of the chosen frequency's response is performed, and the resulting data is used in the solution of two linear equations, and finally the reduced order system is constructed.

VI. COMPUTATIONAL RESULTS

We will now demonstrate the performance of our proposed algorithms with numerical examples. In each of the following figures, we use the so-called ‘‘ISS’’ model as the input system, which is a 3-input, 3-output, 270-state flexural model of one of the modules found on the International Space Station [13]. The code that generated these figures may be found at the GitHub repository <https://github.com/bluesun212/ITFramework>.

Additionally, we use the square root of the trace of the covariance matrix of the error system (or an approximation thereof) as an indicator of the approximation performance, which we denote ‘‘error norm’’ in the figures. This measures the error across the entire frequency spectrum and is identical to the H_2 norm of the error system for stable systems.

Fig. 1 shows the error norm plotted against the reduced systems' state dimension for a number of algorithms, namely balanced truncation, the Loewner framework, tangential-AAA, and our proposed method using the maximum error frequency selection approach. Up until about 20 states, each of the methods perform similarly. After that, our proposed method sees continued improvement as the the number of states increases, and remains close to balanced truncation's.

We now compare the performance of each of our frequency selection methods, starting with the gridded strategy as shown in Fig. 2. In each iteration of the gridded approach, an interpolation point is added at the frequency of maximum error among a grid of $K = 50, 200,$ and 500 logarithmically spaced points between $[10^{-1}, 10^2]$. We see that performance is very good with $K = 200$ and nearly identical to that of the

Algorithm 5 The low-rank tangential algorithm

Require: State space system G , μ , ρ

Require: K , ω_{\min} , ω_{\max} , $\{\hat{\omega}_k\}_{k=1}^K$ depending on algorithm

- 1: $R \leftarrow D, k \leftarrow 1$
- 2: Initialize empty $\mathcal{A}, \mathcal{B}_m, \mathcal{B}_n, \mathcal{C}_\ell$
- 3: $\Theta \leftarrow$ the controllability Gramian of G
- 4: **repeat**
- 5: Use one of Algorithms 1-3 to get ω
- 6: Use Algorithm 4 to compute $\omega, r_{\min}, r_{\max}$
- 7: $U_k, \Sigma_k, V_k \leftarrow$ the r_{\min} th to r_{\max} th singular values/vectors from the SVD of $G(j\omega)$
- 8: Solve $C_k(j\omega I - A) = U_k^* C$ for C_k
- 9: **if** G complex or $\omega = 0$ **then**
- 10: Diagonally concatenate $[j\omega I]$ to \mathcal{A}
- 11: Vertically concatenate $[U_k^*]$ to \mathcal{B}_m
- 12: Vertically concatenate $[\Sigma_k V_k^*]$ to \mathcal{B}_n
- 13: Vertically concatenate $[C_k]$ to \mathcal{C}_ℓ
- 14: **else**
- 15: Diagonally concatenate $\begin{bmatrix} 0 & \omega I \\ -\omega I & 0 \end{bmatrix}$ to \mathcal{A}
- 16: Vertically concatenate $\begin{bmatrix} \Re(U_k)^T \\ \Im(U_k)^T \end{bmatrix}$ to \mathcal{B}_m
- 17: Vertically concatenate $\begin{bmatrix} \Sigma_k \Re(V_k)^T \\ \Sigma_k \Im(V_k)^T \end{bmatrix}$ to \mathcal{B}_n
- 18: Vertically concatenate $\begin{bmatrix} \Re(C_k) \\ \Im(C_k) \end{bmatrix}$ to \mathcal{C}_ℓ
- 19: Solve $\mathbb{W} \mathcal{C}_\ell \Theta \mathcal{C}_\ell^* = C \Theta \mathcal{C}_\ell^*$ for \mathbb{W}
- 20: $R \leftarrow \begin{bmatrix} \mathcal{A} - \mathcal{B}_m \mathbb{W} & \mathcal{B}_n - \mathcal{B}_m D \\ \mathbb{W} & D \end{bmatrix}$
- 21: **until** R sufficiently approximates G

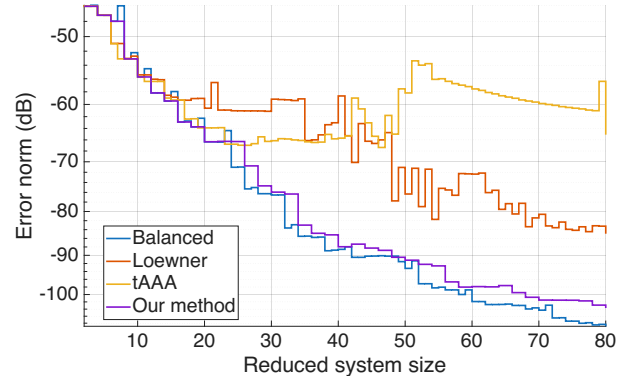


Fig. 1: A comparison of the performance of balanced reduction in blue, the generalized Loewner framework [5] in red, the tangential-AAA (tAAA) algorithm [11] in yellow, and one of our proposed methods (max. error algorithm) in purple. The tAAA algorithm and the Loewner framework both were provided an input set of 1000 points logarithmically spaced between $\pm[10^{-1}, 10^2]j$. The graph shows the norm of the error system versus the reduced system's number of poles. The input model is the 3-input, 3-output, 270-state ‘‘ISS’’ model [13].

maximum error approach with $K = 1000$. A grid with many points is required in order to accurately resolve fine details.

A comparison of random strategy, which selects the frequency of highest error from K logarithmically sampled points between $[10^{-1}, 10^2]$, is shown in Fig. 3. For $K = 5, 20,$ and 100 , we reduced the ISS system and recorded the error norm for 500 different random starting seeds. The mean behavior of these trials and the middle 50% performance is shown in Fig. 3 in comparison to the maximum frequency approach. We

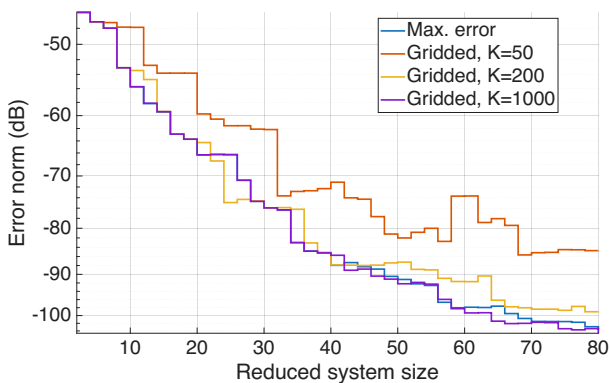


Fig. 2: A comparison of the performance of the maximum error strategy (in blue) and the gridded frequency point selection (in varying colors) with varying K , the number of points in the grid.

note as K increases, the average performance increases and the variance among runs decreases. When $K = 20$, the mean behavior is markedly better than that of $K = 5$, and when $K = 100$, the mean performance practically identical to the maximum error approach.

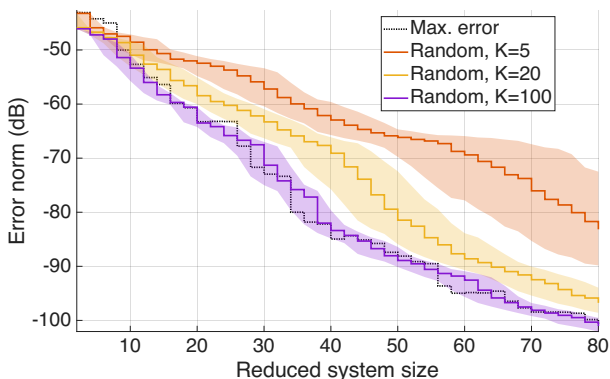


Fig. 3: A comparison of the performance of the maximum error strategy (in black) and random frequency point selection strategy (in varying colors) with varying K , the number of points tested per iteration, versus reduced system size. The solid lines represent the mean behavior of a number of random runs, with the shaded regions representing the middle 50% behavior.

We note that the mean random approach requires an order of magnitude fewer points than the gridded approach, but the performance is non-deterministic, which is an important trade-off the end-user will have to consider when selecting the most appropriate algorithm. Nevertheless, these two figures indicate that good performance can be attained with less computational power required compared to the maximum error approach. To bolster this point, we compare the qualitative performance of each algorithm in Fig. 4. The diamonds on each line show the interpolated frequencies for each of the proposed algorithms after three iterations. The maximum error approach evidently interpolates at the frequency with maximum error, which tends to be located at a peak in the frequency response. The gridded approach generally interpolates at the closest grid point to these peaks, and the random approach behaves non-deterministically. Despite not interpolating at the position of maximum error, the reduced order models the latter two algorithms produce still manage to replicate the response of the system at the peaks well, which is due to the weight

optimization ensuring a proxy for the error across the entire frequency domain is minimized.

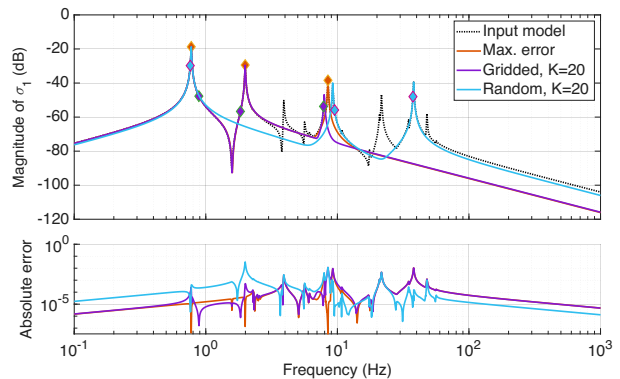


Fig. 4: A plot of the maximum singular value (σ_1) of the unreduced input model and each of our proposed algorithms reduced to 6 states on the upper sub-figure, along with the absolute error in the bottom sub-figure. In the top figure, the dotted black line indicates σ_1 of the input system, which is the aforementioned “ISS” model. In both plots, the maximum error approach is in red, the gridded approach is in purple, and the random approach is in blue. The diamonds indicate where the matching algorithm placed an interpolation point. The gridded approach uses a set of 20 frequencies logarithmically spaced between $[10^{-1}, 10^2]$. The random approach selects the best frequency of 20 random frequencies between $[10^{-1}, 10^2]$.

One important aspect not demonstrated in the figures is the stability of the resulting system. Moment matching methods are not guaranteed to produce a stable model even if the input model is stable; in fact, the models produced by the Loewner framework and the tangential-AAA algorithm are generally unstable. In comparison, the models produced from our algorithms tend to have good stability characteristics, including for systems beside the ISS system.

VII. DISCUSSION AND CONCLUSION

In this work we have introduced an algorithm based on the AAA algorithm and the Loewner framework for the model reduction of MIMO systems. We derived a state-space representation of the tangential interpolant which is constructed from frequency response data and a free parameter matrix. This free parameter matrix is the solution of an optimization problem and has a closed form solution which can be found by solving a linear equation. Importantly, this choice of free parameters ensures that a weighted H_2 norm of the error is decreasing and reaches 0 when the resulting system’s state dimension equals the number of observable and controllable modes of the original system. We discussed the method of interpolation frequency selection and introduced three algorithms, each of which trade off approximation performance with computational complexity. The numerical examples demonstrated good performance on par with standard model reduction methods and improved performance compared to other moment matching methods including good stability characteristics.

In future works we plan to adapt this algorithm for use on sparse systems and explore more sophisticated frequency selection methods. We also plan to prove more theoretical properties including stability characteristics, the existence of monotonically decreasing upper bounds for the H_2 and H_∞ norms of the error system, and expressions describing the improvement across iterations.

APPENDIX I

Assumption 1: Consider the system G , let $\{\omega_i\}_{i=1}^\ell$ be a set of distinct real numbers, and let $\{r_i\}_{i=1}^\ell$ be a set of ranks. Consider the rank- r_i -truncated SVD of $G(\cdot)$ at each $j\omega_i$ where r_i is less than or equal to the rank of $G(j\omega_i)$, i.e. $U_i \Sigma_i V_i^*$ forms the best rank- r_i approximation of $G(j\omega_i)$. Under these assumptions, we have $U_i \in \mathbb{C}^{p \times r_i}$, $U_i^* U_i = I$, diagonal full-rank $\Sigma_i \in \mathbb{R}^{r_i \times r_i}$, $V_i \in \mathbb{C}^{q \times r_i}$, and $V_i^* V_i = I$.

Theorem 3.1: Consider the assumptions in Assumptions 1 and the interpolant R from equation (2), where each $W_i \in \mathbb{C}^{p \times r_i}$, $i = 1, \dots, \ell$ is a full-column-rank free parameter. Then, R left-interpolates G at each $j\omega_i$ for any valid weight $W_i \in \mathbb{C}^{p \times r_i}$, and $\lim_{|s| \rightarrow \infty} R(s) = D$.

Proof: Consider the interpolant from equation (2)

$$\begin{aligned} R(s) &:= M^{-1}(s)N(s) := ([I \ W] \mathcal{M}(s))^{-1} [I \ \mathbb{W}] \mathcal{N}(s) \\ &:= \left(I + \sum_{k=1}^{\ell} \frac{W_k U_k^*}{s - j\omega_k} \right)^{-1} \left(D + \sum_{k=1}^{\ell} \frac{W_k \Sigma_k V_k^*}{s - j\omega_k} \right). \end{aligned}$$

Let $G(j\omega_i) = U_i \Sigma_i V_i^* + U_i^\perp$, where $U_i^* U_i^\perp = 0$. Then, $U_i^* G(j\omega_i) = \Sigma_i V_i^*$. M^{-1} exists because it is a proper square system with invertible feedthrough term, thus $M(s)R(s) = N(s)$ at all but a finite number of points. Expanding M and N and multiplying by $s - j\omega_i$ yields the relation

$$\begin{aligned} \left((s - j\omega_i)I + W_i U_i^* + \sum_{k=1, k \neq i}^{\ell} \frac{(s - j\omega_i)W_k U_k^*}{s - j\omega_k} \right) R(s) &= \\ \left((s - j\omega_i)D + W_i \Sigma_i V_i^* + \sum_{k=1, k \neq i}^{\ell} \frac{(s - j\omega_i)W_k \Sigma_k V_k^*}{s - j\omega_k} \right). \end{aligned}$$

Letting $s = j\omega_i$, all terms containing $s - j\omega_i$ vanish, giving

$$W_i U_i^* R(j\omega_i) = W_i \Sigma_i V_i^* \implies W_i (U_i^* R(j\omega_i) - \Sigma_i V_i^*) = 0.$$

Because W_i is full column rank, it has a trivial null-space, thus $U_i^* R(j\omega_i) - \Sigma_i V_i^* = 0$, and $U_i^* R(j\omega_i) = U_i^* G(j\omega_i)$. Taking the limit as $|s| \rightarrow \infty$ of equation (2), all terms in the sum approach zero, thus $\lim_{|s| \rightarrow \infty} R(s) = D$. ■

Theorem 3.3: Suppose $H = \mathcal{N} - \mathcal{M}G$, where

$$\mathcal{M} = \begin{bmatrix} I \\ M_1(s) \\ \vdots \\ M_\ell(s) \end{bmatrix}, \quad \mathcal{N} = \begin{bmatrix} D \\ N_1(s) \\ \vdots \\ N_\ell(s) \end{bmatrix}, \quad \text{and}$$

$$[M_k \ N_k] = \begin{cases} \begin{bmatrix} j\omega_k I & U_k^* & \Sigma_k V_k^* \\ I & 0 & 0 \end{bmatrix} & \text{if } G \text{ complex or } \omega_k = 0 \\ \begin{bmatrix} 0 & \omega_k I & \Re(U_k^T) & \Sigma_k \Re(V_k^T) \\ -\omega_k I & 0 & \Im(U_k^T) & \Sigma_k \Im(V_k^T) \\ I & 0 & 0 & 0 \\ 0 & I & 0 & 0 \end{bmatrix} & \text{o.w.} \end{cases}$$

Then the system H has the realization

$$H = \left[\begin{array}{c|c} A & B \\ \hline -C & 0 \\ \mathcal{C}_\ell & 0 \end{array} \right], \quad \mathcal{C}_\ell = \begin{bmatrix} C_1 \\ \vdots \\ C_\ell \end{bmatrix} \in \mathbb{C}^{r \times n}, \quad (19)$$

and

$$C_k = \begin{cases} U_k^* C(j\omega_k I - A)^{-1} & \text{if } G \text{ complex or } \omega_k = 0 \\ \begin{bmatrix} \Re(U_k^* C(j\omega_k I - A)^{-1}) \\ -\Im(U_k^* C(j\omega_k I - A)^{-1}) \end{bmatrix} & \text{o.w.} \end{cases}$$

Proof: Consider the system H in block column form

$$H = \begin{bmatrix} H_0 \\ H_1 \\ \vdots \\ H_\ell \end{bmatrix} = \begin{bmatrix} D-G \\ \mathcal{N}_1 - \mathcal{M}_1 G \\ \vdots \\ \mathcal{N}_\ell - \mathcal{M}_\ell G \end{bmatrix}.$$

The first block system H_0 has the realization

$$H_0 = \left[\begin{array}{c|c} A & B \\ \hline -C & 0 \end{array} \right]. \quad (20)$$

Now suppose that H_k is associated with the interpolation point at $\omega_k = 0$, or any frequency in the case that G has complex coefficients. The dynamical system describing H_k can be written as

$$\begin{aligned} \dot{x} &= Ax + Bu \\ \dot{z}_1 &= j\omega_k z_1 + \Sigma_k V_k^* u \\ \dot{z}_2 &= U_k^* Cx + j\omega_k z_2 + U_k^* D u \\ y &= z_1 - z_2. \end{aligned}$$

Now we let $z = z_1 - z_2$, which yields

$$\begin{aligned} \dot{x} &= Ax + Bu \\ \dot{z} &= -U_k^* Cx + j\omega_k z + (\Sigma_k V_k^* - U_k^* D)u \\ y &= z. \end{aligned}$$

Note that the mode $\hat{z} = z_1 + z_2$ is unobservable so it can be discarded. We can utilize the fact that $U_k^* U_k = I$ and $U_k \Sigma_k V_k^* = C(j\omega_k I - A)^{-1} B + D - U_k^\perp$ for some U_k^\perp with $U_k^* U_k^\perp = 0$ to simplify further:

$$\begin{aligned} \dot{z} &= j\omega_k I z - U_k^* (Cx - (U_k \Sigma_k V_k^* - D)u) \\ &= j\omega_k z - U_k^* (Cx - C(j\omega_k I - A)^{-1} B u) + U_k^* U_k^\perp u \\ &= j\omega_k z - U_k^* C(j\omega_k I - A)^{-1} ((j\omega_k I - A)x - Bu) \\ &= j\omega_k z + \underbrace{U_k^* C(j\omega_k I - A)^{-1}}_{C_k} (Ax + Bu - j\omega_k x). \end{aligned}$$

Finally, we perform a coordinate change $w = z - C_k x$ to get

$$\begin{aligned} \dot{x} &= Ax + Bu \\ \dot{w} &= j\omega_k z + C_k (Ax + Bu - j\omega_k x) - C_k (Ax + Bu) \\ &= j\omega_k (z - C_k x) = j\omega_k w \\ y &= C_k x - w. \end{aligned}$$

The w state is uncontrollable, so it can be removed, yielding

$$H_k = \left[\begin{array}{c|c} A & B \\ \hline C_k & 0 \end{array} \right], \quad C_k = U_k^* C(j\omega_k I - A)^{-1} \quad (21)$$

as a state space realization for H_k .

Now consider the case that G has real coefficients and $\omega_k \neq 0$. The structure for \mathcal{M}_k and \mathcal{N}_k is slightly different in this case. Let

$$[\mathcal{M}_k^c \ \mathcal{N}_k^c] = \left[\begin{array}{c|c} j\omega_k I & U_k^* \ \Sigma_k V_k^* \\ \hline I & 0 \ \ 0 \end{array} \right].$$

From Remark 3.1,

$$[\mathcal{M}_k \ \mathcal{N}_k] = \begin{bmatrix} \Re(\mathcal{M}_k^c) & \Re(\mathcal{N}_k^c) \\ -\Im(\mathcal{M}_k^c) & -\Im(\mathcal{N}_k^c) \end{bmatrix},$$

thus by properties of $\Re(\cdot)$ and $\Im(\cdot)$ on systems,

$$\begin{aligned} H_k &= \begin{bmatrix} \Re(\mathcal{N}_k^c) \\ -\Im(\mathcal{N}_k^c) \end{bmatrix} - \begin{bmatrix} \Re(\mathcal{M}_k^c) \\ -\Im(\mathcal{M}_k^c) \end{bmatrix} G \\ &= \begin{bmatrix} \Re(\mathcal{N}_k^c - \mathcal{M}_k^c G) \\ -\Im(\mathcal{N}_k^c - \mathcal{M}_k^c G) \end{bmatrix} = \begin{bmatrix} \Re(H_k^c) \\ -\Im(H_k^c) \end{bmatrix}, \end{aligned}$$

where H_k^c is the H_k matrix that appears in equation (21). Substituting in state space realizations for $\Re(H_k^c)$ and $\Im(H_k^c)$ yields

$$H_k = \left[\begin{array}{cc|c} A & 0 & B \\ 0 & A & 0 \\ \hline \Re(C_k^c) & -\Im(C_k^c) & 0 \\ -\Im(C_k^c) & -\Re(C_k^c) & 0 \end{array} \right],$$

where C_k^c is the C_k that appears in equation (21). The second block state is uncontrollable, so it can be discarded, yielding

$$H_k = \left[\begin{array}{c|c} A & B \\ \hline C_k & 0 \end{array} \right], \quad C_k = \begin{bmatrix} \Re(U_k^* C(j\omega_k I - A)^{-1}) \\ -\Im(U_k^* C(j\omega_k I - A)^{-1}) \end{bmatrix}. \quad (22)$$

We see that in all cases, each H_k has the same ‘‘A’’ and ‘‘B’’ matrices, meaning a realization for H can be created by vertically stacking each of their ‘‘C’’ and ‘‘D’’ matrices, yielding the realization for H is what is stated in the theorem statement. ■

Lemma 1.1: Let

$$G = \left[\begin{array}{c|c} A & B \\ \hline C & D \end{array} \right] \quad \text{and} \quad G_{\min} = \left[\begin{array}{c|c} A_{\min} & B_{\min} \\ \hline C_{\min} & D \end{array} \right],$$

where G_{\min} is a minimal realization of G . Let Θ and Θ_{\min} be the controllability Gramians of G and G_{\min} respectively. Also let

$$\widehat{C} = \begin{bmatrix} \widehat{C}_1 \\ \vdots \\ \widehat{C}_m \end{bmatrix} \quad \text{and} \quad \widehat{C}_{\min} = \begin{bmatrix} \widehat{C}_{1,\min} \\ \vdots \\ \widehat{C}_{m,\min} \end{bmatrix},$$

where $\widehat{C}_k = U_k^* C(s_k I - A)^{-1}$ and $\widehat{C}_{k,\min} = U_k^* C_{\min}(s_k I - A_{\min})^{-1}$. Then $\widehat{C}\Theta\widehat{C}^* = \widehat{C}_{\min}\Theta_{\min}\widehat{C}_{\min}^*$, $C\Theta\widehat{C}^* = C_{\min}\Theta_{\min}\widehat{C}_{\min}^*$ and $C\Theta C^* = C_{\min}\Theta_{\min}C_{\min}^*$.

Proof: First, note the integral forms

$$\begin{aligned} \widehat{C}\Theta\widehat{C}^* &= \int_0^\infty \widehat{C}\theta(j\omega)\theta^*(j\omega)\widehat{C}^* d\omega \\ C\Theta\widehat{C}^* &= \int_0^\infty C\theta(j\omega)\theta^*(j\omega)\widehat{C}^* d\omega \\ C\Theta C^* &= \int_0^\infty C\theta(j\omega)\theta^*(j\omega)C^* d\omega \end{aligned}$$

where $\theta(s) = (sI - A)^{-1}B$. Consider the similarity transformation T^{-1} on G yielding the canonical Kalman decomposition [14], i.e.

$$A = T^{-1} \begin{bmatrix} A_{\min} & 0 & A_{\times o} & 0 \\ A_{c \times} & A_{c \bar{o}} & A_{\times \times} & A_{\times \bar{o}} \\ 0 & 0 & A_{\bar{o} 0} & 0 \\ 0 & 0 & A_{\bar{o} \times} & A_{\bar{o} \bar{o}} \end{bmatrix} T, \quad B = T^{-1} \begin{bmatrix} B_{\min} \\ B_{c \bar{o}} \\ 0 \\ 0 \end{bmatrix},$$

$$C = [C_{\min} \ 0 \ C_{\bar{o} 0} \ 0]T.$$

Note that the symbol \times denotes a quantity that is unimportant for the proof. Applying this transformation on $(sI - A)^{-1}$ yields

$$(sI - A)^{-1} = T^{-1} \begin{bmatrix} (sI - A_{\min})^{-1} & 0 & \times & 0 \\ \times & (sI - A_{c \bar{o}})^{-1} & \times & \times \\ 0 & 0 & (sI - A_{\bar{o} 0})^{-1} & 0 \\ 0 & 0 & \times & (sI - A_{\bar{o} \bar{o}})^{-1} \end{bmatrix} T,$$

thus

$$\begin{aligned} \widehat{C}_k &= [U_k^* C_{\min}(s_k I - A_{\min})^{-1} \ 0 \times 0]T = [\widehat{C}_{k,\min} \ 0 \times 0]T, \\ \widehat{C} &= [\widehat{C}_{\min} \ 0 \times 0]T, \quad \text{and} \\ \theta(s) &= T^{-1} \begin{bmatrix} (sI - A_{\min})^{-1} B_{\min} \\ \times \\ 0 \\ 0 \end{bmatrix} =: T^{-1} \begin{bmatrix} \theta_{\min}(s) \\ \times \\ 0 \\ 0 \end{bmatrix}. \end{aligned}$$

From this, it is evident that $C\theta(s) = C_{\min}\theta_{\min}(s)$ and $\widehat{C}\theta(s) = \widehat{C}_{\min}\theta_{\min}(s)$. Substituting these back into the integrals, factoring out C_{\min} and \widehat{C}_{\min} , and replacing the integrals with the Gramian Θ_{\min} yields the equalities. ■

Lemma 1.2: Let

$$\widehat{C} = \begin{bmatrix} U_1^* C(s_1 I - A)^{-1} \\ \vdots \\ U_m^* C(s_m I - A)^{-1} \end{bmatrix} \in \mathbb{C}^{r \times n},$$

where $A \in \mathbb{C}^{n \times n}$ and $C \in \mathbb{C}^{p \times n}$. Assume each s_k is distinct and not an eigenvalue of A , each $U_k \in \mathbb{C}^{p \times r_i}$ is full rank, each block row is individually full rank, and the pair (C, A) is observable. Additionally, if $r \geq n$, then assume $\text{rank}[U_1 \ \dots \ U_m] = p$. Then, $\text{rank}(\widehat{C}) = \min(r, n)$.

Proof: First, we can write \widehat{C} as the solution of a Sylvester equation. Indeed,

$$\underbrace{\begin{bmatrix} s_1 I_{r_1} & & \\ & \ddots & \\ & & s_m I_{r_m} \end{bmatrix}}_S \widehat{C} - \widehat{C}A = \underbrace{\begin{bmatrix} U_1^* \\ \vdots \\ U_m^* \end{bmatrix}}_{U^*} C.$$

This becomes clear when checking a block row of the Sylvester equation:

$$\begin{aligned} s_k I_{r_k} U_k^* C(s_k I_n - A)^{-1} - U_k^* C(s_k I_n - A)^{-1} A &= U_k^* C \\ U_k^* C(s_k I_n - A)^{-1} (s_k I_n - A) &= U_k^* C. \end{aligned}$$

The eigenvalues of S are s_1 through s_m which we assumed are not eigenvalues of A , thus due to Lemma 1.3, we see \widehat{C} has a unique solution.

If $r \leq n$, then \widehat{C} is full row rank when (S, U^*C) is controllable, which we can see from the PBH test for controllability, i.e. for all eigenvalues of S λ , $\text{rank}[s - \lambda I \ U^*C] = r$. Let $\lambda = s_k$, then $S - s_k I$ drops rank by r_k because the k th block row of S (the row containing s_k) becomes zero. However, the k th block row of U^*C is U_k^*C which is full rank because we assumed each $U_k^*C(s_k I - A)^{-1}$ was, thus the matrix $[s - \lambda I \ U^*C]$ is always full row rank and the pair (S, U^*C) is controllable.

If $r \geq n$, then \widehat{C} is full column rank when (U^*C, A) is observable. We can show this using the PBH test for observability. Indeed, consider the matrix

$$\begin{bmatrix} A - \lambda I \\ U^*C \end{bmatrix} = \begin{bmatrix} I & 0 \\ 0 & U^* \end{bmatrix} \begin{bmatrix} A - \lambda I \\ C \end{bmatrix}.$$

Suppose U has full column rank, i.e. $\text{rank} U = p$. Then $\text{rank} \begin{bmatrix} I & 0 \\ 0 & U^* \end{bmatrix} = n + p$, and because the pair (C, A) is observable, $\text{rank} \begin{bmatrix} A - \lambda I \\ C \end{bmatrix} = n$ for all λ . Applying Sylvester’s rank inequality, we get

$$\text{rank} \begin{bmatrix} A - \lambda I \\ U^*C \end{bmatrix} \geq (p + n) + n - (p + n) = n,$$

Thus the pair (U^*C, A) is observable. Thus under our assumptions, \widehat{C} is always full rank, i.e. its rank is $\min(r, n)$. ■

Corollary 1.1: Consider the matrix

$$\mathcal{C}_\ell = \begin{bmatrix} C_1 \\ \vdots \\ C_\ell \end{bmatrix}, \quad C_k = \begin{cases} \hat{C}(j\omega_k, U_k) & \text{if } G \text{ complex or } \omega_k = 0 \\ \begin{bmatrix} \Re(\hat{C}(j\omega_k, U_k)) \\ -\Im(\hat{C}(j\omega_k, U_k)) \end{bmatrix} & \text{o.w.} \end{cases}$$

where $\hat{C}(s, U) = U^* C (sI - A)^{-1}$ and $\mathcal{C}_\ell \in \mathbb{C}^{r \times n}$. Let

$$\mathcal{C}_{\ell, \min} = \begin{bmatrix} C_{1, \min} \\ \vdots \\ C_{\ell, \min} \end{bmatrix} \in \mathbb{C}^{r \times n_{\min}},$$

$$C_{k, \min} = \begin{cases} \hat{C}_{\min}(j\omega_k, U_k) & \text{if } G \text{ complex or } \omega_k = 0 \\ \begin{bmatrix} \Re(\hat{C}_{\min}(j\omega_k, U_k)) \\ -\Im(\hat{C}_{\min}(j\omega_k, U_k)) \end{bmatrix} & \text{o.w.} \end{cases}$$

Then, under the same assumptions from the previous two lemmas, $\text{rank } \mathcal{C}_\ell = \text{rank } \mathcal{C}_{\ell, \min} = \min(r, n_{\min})$, $\mathcal{C}_\ell \Theta_{\mathcal{C}_\ell}^* = \mathcal{C}_{\ell, \min} \Theta_{\mathcal{C}_{\ell, \min}}^*$, and $C \Theta_{\mathcal{C}_\ell}^* = C \Theta_{\mathcal{C}_{\ell, \min}}^*$.

Proof: First, note that when A is real, $\overline{\hat{C}}(s, U) = \overline{U}^* C (\overline{s}I - A)^{-1} = \hat{C}(\overline{s}, \overline{U})$. We can write C_k when $\omega_k \neq 0$ or when G is real as

$$\begin{bmatrix} \Re(\hat{C}(j\omega_k, U_k)) \\ -\Im(\hat{C}(j\omega_k, U_k)) \end{bmatrix} = \begin{bmatrix} \frac{1}{2}(\hat{C}(j\omega_k, U_k) + \overline{\hat{C}}(j\omega_k, U_k)) \\ \frac{1}{2j}(\hat{C}(j\omega_k, U_k) - \overline{\hat{C}}(j\omega_k, U_k)) \end{bmatrix}$$

$$= \begin{bmatrix} \frac{1}{2} & \frac{1}{2} \\ -\frac{1}{2j} & \frac{1}{2j} \end{bmatrix} \begin{bmatrix} \hat{C}(j\omega_k, U_k) \\ \hat{C}(-j\omega_k, \overline{U}_k) \end{bmatrix} =: J_k C_k.$$

In the case that G is complex or $\omega_k = 0$, $J_k = I$ and $C_k = \hat{C}(j\omega_k, U_k)$. Thus, $\mathcal{C}_\ell = J \hat{C}$, where $J \in \mathbb{C}^{r \times r} := \text{diag}(J_1, \dots, J_\ell)$ and

$$\hat{C} \in \mathbb{C}^{r \times n} := \begin{bmatrix} \hat{C}_1 \\ \vdots \\ \hat{C}_m \end{bmatrix}.$$

Note the reindexing of \hat{C} , which highlights the splitting up of each C_k so that each \hat{C}_k corresponds to one point on the imaginary axis. In clearer words, when $\omega_k \neq 0$ or G is real, the corresponding C_k is split into two \hat{C}_k s, one for $j\omega_k$ and one for $-j\omega_k$.

Given that J is invertible, $\text{rank } \mathcal{C}_\ell = \text{rank } \hat{C}$. Utilizing an intermediate result from Lemma 1.1, we have

$$\text{rank } \hat{C} = \text{rank}([\hat{C}_{\min} \ 0 \times 0]T) = \text{rank } \hat{C}_{\min},$$

which is equal to $\min(r, n_{\min})$ according to Lemma 1.2 because the pair (C_{\min}, A_{\min}) is observable, thus $\text{rank } \mathcal{C}_\ell = \min(r, n_{\min})$.

In addition to this, let $\mathcal{C}_{\ell, \min} := J \hat{C}_{\min}$. Then,

$$\mathcal{C}_\ell \Theta_{\mathcal{C}_\ell}^* = J \hat{C}_{\min} \Theta_{\mathcal{C}_{\ell, \min}}^* J^* = \mathcal{C}_{\ell, \min} \Theta_{\mathcal{C}_{\ell, \min}}^*,$$

$$C \Theta_{\mathcal{C}_\ell}^* = J C \Theta_{\mathcal{C}_{\ell, \min}}^* J^* = C_{\min} \Theta_{\mathcal{C}_{\ell, \min}}^*$$

as required. ■

Lemma 1.3: [15] Consider the Sylvester equation

$$A_1 X - X A_2 = B$$

where $A_1 \in \mathbb{C}^{r \times r}$, $A_2 \in \mathbb{C}^{n \times n}$, $X \in \mathbb{C}^{r \times n}$, and $B \in \mathbb{C}^{r \times n}$. If there are no shared eigenvalues between A_1 and A_2 , then a unique solution for X exists. Furthermore, if $r \leq n$ and the pair (A_1, B) is controllable, then X is full row rank. If $r \geq n$, then X is full column rank if the pair (B, A_2) is observable. If $r = n$, then both must be true.

REFERENCES

- [1] D. Rafiq and M. A. Bazaz, "Model order reduction via moment-matching: a state of the art review," *Archives of Computational Methods in Engineering*, vol. 29, no. 3, pp. 1463–1483, 2022.
- [2] T. Lassila, A. Manzoni, A. Quarteroni, and G. Rozza, *Model Order Reduction in Fluid Dynamics: Challenges and Perspectives*. Cham: Springer International Publishing, 2014, pp. 235–273.
- [3] U. Hetmaniuk, R. Tezaur, and C. Farhat, "Review and assessment of interpolatory model order reduction methods for frequency response structural dynamics and acoustics problems," *International Journal for Numerical Methods in Engineering*, vol. 90, no. 13, pp. 1636–1662, 2012.
- [4] A. C. Antoulas and B. D. Q. Anderson, "On the scalar rational interpolation problem," *IMA Journal of Mathematical Control and Information*, vol. 3, no. 2-3, 1986.
- [5] A. C. Antoulas, S. Lefteriu, A. C. Ionita, P. Benner, and A. Cohen, "A tutorial introduction to the loewner framework for model reduction," *Model Reduction and Approximation: Theory and Algorithms*, vol. 15, p. 335, 2017.
- [6] Y. Nakatsukasa, O. Sète, and L. N. Trefethen, "The AAA algorithm for rational approximation," *SIAM Journal on Scientific Computing*, vol. 40, no. 3, pp. A1494–A1522, jan 2018.
- [7] A. C. Antoulas, C. A. Beattie, and S. Gügürcin, *Interpolatory Methods for Model Reduction*. Philadelphia, PA: Society for Industrial and Applied Mathematics, 2020.
- [8] S. Gugercin, "An iterative SVD-Krylov based method for model reduction of large-scale dynamical systems," *Linear Algebra and its Applications*, vol. 428, no. 8, pp. 1964–1986, 2008.
- [9] A. Yu and A. Townsend, "Leveraging the Hankel norm approximation and data-driven algorithms in reduced order modeling," *Numerical Linear Algebra with Applications*, vol. 31, no. 4, p. 2555, 2024.
- [10] J. Jonas and B. Bamieh, "An adaptation of the AAA-interpolation algorithm for model reduction of MIMO systems," in *2024 American Control Conference (ACC)*, ser. 2024 American Control Conference (ACC). IEEE, 2024.
- [11] Q. Aumann, P. Benner, I. V. Gosea, J. Saak, and J. Vettermann, "A tangential interpolation framework for the AAA algorithm," *PAMM*, vol. 23, no. 3, p. e202300183, 2023.
- [12] N. Bruinsma and M. Steinbuch, "A fast algorithm to compute the H_∞ -norm of a transfer function matrix," *Systems & Control Letters*, vol. 14, no. 4, pp. 287–293, 1990.
- [13] Y. Chahlaoui, "Benchmark examples for model reduction." [Online]. Available: <http://slicot.org/20-site/126-benchmark-examples-for-model-reduction>
- [14] J. P. Hespanha, *Linear Systems Theory*. Princeton, New Jersey: Princeton Press, Feb. 2018.
- [15] E. de Souza and S. Bhattacharyya, "Controllability, observability and the solution of $AX - XB = C$," *Linear Algebra and its Applications*, vol. 39, pp. 167–188, 1981.



Jared Jonas received a B.Sc. degree in mechanical engineering from California State University, Fullerton in 2019 and a M.Sc. degree in mechanical engineering from University of California, Los Angeles in 2022. After, he joined the department of mechanical engineering at University of California, Santa Barbara where he is currently a Ph.D. candidate. His research interests include computational methods in optimal control, reduced order modeling, and system identification.



Bassam Bamieh (Fellow, IEEE) received the B.Sc. degree in electrical engineering and physics from Valparaiso University, Valparaiso, IN, USA, in 1983, and the M.Sc. and Ph.D. degrees in electrical and computer engineering from Rice University, Houston, TX, USA, in 1986 and 1992, respectively. From 1991 to 1998, he was an Assistant Professor with the Department of Electrical and Computer Engineering, and the Coordinated Science Laboratory, University of Illinois at Urbana-Champaign, after which he

joined the University of California at Santa Barbara (UCSB), where he is currently a Professor of Mechanical Engineering. His research interests include robust and optimal control, distributed and networked control and dynamical systems, and related problems in fluid and statistical mechanics and thermoacoustics. Dr. Bamieh is a past recipient of the IEEE Control Systems Society G. S. Axelby Outstanding Paper Award (twice), the AACC Hugo Schuck Best Paper Award, and the National Science Foundation CAREER Award. He was a Distinguished Lecturer of the IEEE Control Systems Society (twice), and is a Fellow of the International Federation of Automatic Control (IFAC).